Nanoscale

Cite this: *Nanoscale*, 2012, **4**, 3781

www.rsc.org/nanoscale

**PAPER**

# Chemical modification of graphene characterized by Raman and transport experiments†

**Fabian M. Koehler,‡[a] Arnhild Jacobsen,‡[b] Thomas Ihn,[b] Klaus Ensslin[b] and Wendelin J. Stark*[a]**

***Received 15th February 2012, Accepted 19th April 2012***
**DOI: 10.1039/c2nr30364g**



A chemical approach to modify the electronic transport of graphene is investigated by detailed transport and Raman spectroscopy measurements on Hall bar shaped samples. The functionalization of graphene with nitrobenzene diazonium ions results in a strong p-doping of the graphene samples and only slightly lower mobilities. Comparing Raman and transport data taken after each functionalization step allowed the conclusion that two preferential reactions take place on the graphene surface. In the beginning a few nitrobenzene molecules are directly attached to the graphene atoms creating defects. Afterwards these act as seeds for a polymer like growth not directly connected to the graphene atoms. The effects of solvents were excluded by thorough control measurements.

## 1 Introduction

Chemical modifications of graphene have resulted in a plethora of graphene derivatives ranging from simply hydrogenated and fluorinated graphene[1–3] to polymer functionalized graphene flakes in solutions.[4]

Due to its high mobilities graphene is considered as a promising candidate for the next generation of electronics. However, a problematic issue with electronic graphene devices is the absence of a band gap in this material. So far, a so-called transport gap has been realized by confining the charge carriers in narrow ribbons.[5–7] This allows the suppression of current flow by gating; however, the tunability of the resulting tunnel barriers is poor. Therefore, it would be desirable to find an alternative route to open a band gap in graphene. One possible approach would be to use bilayer graphene where it has been shown that a gate tunable band gap can be opened when the symmetry between the two layers is broken.[8–11] However, there are still challenges that have to be solved in order to exploit this band gap for devices.

Another suggested approach is chemical functionalization.[2,3,12–14] This approach is especially interesting because it is easy to implement and, in addition to the opening of a band gap, it might also offer the possibility for controlled doping of graphene. Furthermore, chemistry might provide a possibility for specific edge functionalization,[15,16] which would be an interesting tool in combination with existing etching techniques to chemically design the edges of nano-devices.

To explore these possibilities we present a detailed electronic transport and Raman spectroscopy study of the chemical functionalization of single layer graphene Hall bars. The Hall bars are stepwise functionalized by diazonium chemistry, which is a prominent example of chemically modified graphene.[15–20] The resulting surface functionalization consists ideally of nitrobenzene moieties standing perpendicularly to the graphene plane where the connecting carbon atom from graphene is $sp^3$ hybridized.[15,18] However, diazonium reactions involve radical transition states known to result in an unselective product distribution, like polymeric structures.[21]

## 2 Experimental section

Single layer graphene flakes are obtained by mechanical exfoliation of natural graphite. The flakes are deposited onto a silicon substrate covered by 295 nm of $SiO_2$ where the highly doped silicon serves as a global backgate for the electronic transport measurements. The single layer nature of the flakes is confirmed by optical microscopy and Raman spectroscopy. In a first electron beam lithography step followed by metal evaporation (5 nm Ti/40 nm Au) the Ohmic contacts are defined. In a second electron beam lithography step the Hall bar structure is patterned and subsequently cut out by reactive ion etching.

The devices are functionalized at room temperature by immersing the whole chip into a 20 mmol $L^{-1}$ solution of water-soluble nitrobenzene diazonium salt (4-nitrobenzene diazonium tetrafluorborate from Sigma Aldrich). Afterwards the chip is cleaned in isopropanol and blown dry with nitrogen. In the first functionalization step the chip is immersed for 1 minute. In the following 5 functionalization steps the immersion time is

[a]*Institute for Chemical and Bioengineering, Department of Chemistry and Applied Biosciences, ETH Zurich, 8093 Zurich, Switzerland. E-mail: wendelin.stark@chem.ethz.ch; Fax: +41 44 633 10 83; Tel: +41 44 632 09 80*
[b]*Solid State Physics Laboratory, Department of Physics, ETH Zurich, 8093 Zurich, Switzerland*

† Electronic supplementary information (ESI) available: Additional Raman data. See DOI: 10.1039/c2nr30364g

‡ Both authors have contributed equally to this work.

increased to 5, 20, 40 and 100 minutes, respectively. Note that in the following we will refer to the total functionalization time which is 1, 6, 26, 66 and 166 minutes respectively.

## 3 Results and discussion

In a previous study it has been shown that immersing a chip in pure water and isopropanol leads to doping similar to the doping effect expected from the functionalization.[19] Here, we have therefore performed a control experiment where the chip is first immersed only in water and isopropanol. As in the previous study a strong p-doping is observed. However, by heating the sample in vacuum at around 100 °C for approximately two days the dopants originating from the solvents could be removed. As a consequence this heating step is performed after each functionalization step and the transport measurements are performed right afterwards without breaking the vacuum. We therefore assume that the doping observed in the following data is not due to solvent effects, but only due to diazonium moieties, either covalently bonded to or absorbed on the graphene surface. To complement the transport data the Hall bars were also thoroughly investigated by Raman spectroscopy after each functionalization step. The Raman spectroscopy measurements were always performed after the transport measurements and at ambient conditions. The laser power was kept below 2 mW to avoid heating and laser induced defects.

Two Hall bars were measured in parallel in this study and the obtained results are qualitatively the same. In the following we will present the measurements obtained from the Hall bar depicted in Fig. 1(a). The transport measurements are performed by applying a constant current of 10 nA through the Hall bar while measuring the 4-point longitudinal resistance ($R_{xx}$) and transverse resistance ($R_{xy}$) as shown schematically in Fig. 1(a). In Fig. 1(b), $R_{xx}$ is shown as a function of applied backgate voltage ($V_{BG}$) after the different functionalization steps. For the untreated Hall bar the charge neutrality point (CNP) is at 0 V in backgate and the mobility is determined to be 9000 $cm^2\ V^{-1}\ s^{-1}$ at a density of $1.6 \times 10^{12}\ cm^{-2}$, indicating low initial doping and high quality. For each functionalization step the CNP moves to more positive backgate voltages and the mobility decreases, as can be seen by the increased width of the resistance peak. After 166 minutes of functionalization the CNP is at 45 V and the mobility is decreased to 3200 $cm^2\ V^{-1}\ s^{-1}$. This is comparable to normally observed mobilities for untreated devices with the CNP at similar backgate voltages due to unremoved dopants from the fabrication steps.

The observed shift of the CNP can be explained by the functional group either attached to or adsorbed on the graphene structure. In both cases the functional group acts as a hole dopant. The nitro-benzene group is an electron acceptor, removing electrons from graphene,[18,19] therefore shifting the CNP to more positive backgate potentials. The doping contribution of one perpendicularly oriented nitrobenzene molecule to graphene can be roughly estimated by the dipole moment (4-nitrobenzene ≈ 4.5 D (Debye)) and the assumption of a distance between the graphene plane and the chemical group ($d \approx 0.5$–1 nm). This evaluation leads to a removal of around 0.05 to 0.2 electrons/nitrobenzene molecule from the graphene plane. The removal of electrons is due to the dipole moment pointing towards the graphene plane which essentially is a result of the electron acceptor qualities of the nitrobenzene molecule. In the case of the adsorbed species an estimation of the electrons/nitrobenzene removed is harder, as the final conformation is generally unknown and multilayer adsorption is possible. In general the adsorbed species are closer to the surface and can build charge transfer complexes, therefore more electrons/molecule can be removed from graphene than in the covalently attached case.

The observed change in mobility can also be a result of both induced defects and of charged impurities close to the graphene surface. This has been shown in several previous reports dealing with potassium atoms as dopants,[22] defects through ion irradiation,[23] polymers as dopants[24] or defects through covalently bound molecules[17,24] on the surface of graphene.

To further understand the measurements presented in Fig. 1(b) and to differentiate between the effect of the functional groups as defects or as dopants we plot the minimum conductivity ($\sigma_{min}$) as a function of mobility ($\mu$) for all the functionalization steps. Previously it has been shown by Chen *et al.* in ref. 23 that $\sigma_{min}$ decreases with decreasing $\mu$ when defects are induced in the graphene lattice. However, when only dopants are introduced the ratio stays constant. Here, it can be seen that $\sigma_{min}$ decreases slightly from pristine graphene (high mobility) after the first functionalization step. After further functionalization steps it hardly changes anymore. Following the results of Chen *et al.* the decrease in mobility that we observe is therefore mainly due to doping and only slightly due to the creation of defects.

In addition to electronic transport experiments, Raman spectroscopy is also used to investigate the changes of the graphene

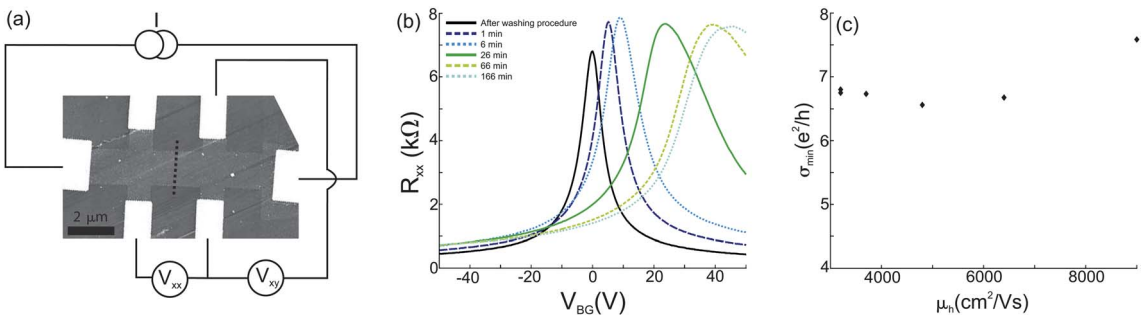


**Fig. 1** Room temperature measurements of functionalized graphene. (a) Processed single layer graphene with Hall bar shape and metal contacts (white). Electrical circuit used for transport measurements is depicted. (b) Backgate sweeps of the device from (a) after each functionalization step. (c) Minimum conductivity *versus* mobility for the functionalization process.

 

during functionalization. Fig. 2(a) shows the Raman spectra of the pristine Hall bar, after 1 minute of functionalization and after 166 minutes of functionalization. Three main peaks can be seen, the D-peak (due to defects), the G-peak and the 2D-peak.[25] For pristine graphene no D-peak is observed. After functionalization a small D-peak occurs, showing that some defects are indeed induced into the graphene lattice. However, the D peak only increases until 26 minutes functionalization time and then it saturates, indicating that defects are only induced in the first functionalization steps. In addition, a shift of the G-peak to higher wavenumbers and a decrease in G/2D ratio is observed for increased functionalization, both known effects of doping.[26,27] These doping effects increase until the last functionalization step, thereby demonstrating that the amount of dopants on the graphene continues to increase after no additional defects are created. This agrees with the previous understanding of the transport data where doping is the dominant effect seen from the functionalization.

From the ratio of the D-peak and the G-peak a rough estimate of the distance between the attached functional groups, and hence their density, can be made by the empirical formula $L_a$ (nm) = $(2.4 \times 10^{-10})\lambda^4(I_D/I_G)^{-1}$.[28] Lucchese *et al.* reported a slightly modified formula, where $(1/L_a)^2 \approx I_D/I_G$, for small $I_D/I_G$ ratios both formulas yield similar $L_a$ values.[29] After 166 minutes of functionalization we calculate $L_a$ to be ~30 nm. This corresponds to a defect density of $\sim 10^{11}$ cm$^{-2}$. From the position of the CNP after 166 minutes of functionalization we estimate a doping density of $\sim 10^{12}$ cm$^{-2}$, which is one order of magnitude larger than the estimated defect density.

Previous Raman spectroscopy studies of graphene functionalized with diazonium salt has shown a large reactivity of the graphene sheet towards the diazonium reagent.[15,16,20] In this study a rather small reactivity is observed, however, a large doping effect is seen. One likely explanation for this is the formation of dendritic polymers.[30] These polymers may have one or few monomers covalently attached to the graphene plane, therefore showing only a small D peak. However, the whole polymer may contribute to the doping, as it can adsorb to the graphene surface. The adsorption of nitrobenzene groups has been shown to p-dope without establishing a D peak.[18] In addition the adsorbed species may remove more electrons/functional group as they can interact by π-stacking, resulting in charge transfer complexes on the graphene surface. The observed doping can also be a result of diazonium species adsorbed on the surface without being part of a polymer structure. However, this is not very likely due to the thorough rinsing of the chip in isopropanol after the functionalization followed by heating in vacuum for two days as described before.

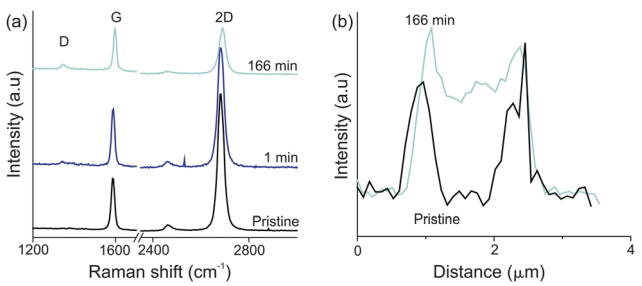


**Fig. 2** (a) Raman spectra of the pristine single layer graphene device and after the first and last functionalization step. (b) Raman line scans over the cross section of the Hall bar device (see dotted line in 2(a)) showing the D peak area as a function of spatial location for the pristine device and after the last functionalization step.

As mentioned before, previous reports have also shown a significantly larger reactivity of graphene edges (D/G ratio ~2) compared to bulk (D/G ratio < = 1) towards diazonium chemistry.[15,16] This is in contrast to the functionalized and measured devices as described in this paper. In Fig. 2(b) line scans of the D-line intensity are shown over the cross section of the Hall bar devices (see dotted line in Fig. 1(a)). Additionally, the D/G ratio is low for both edges and bulk. From these scans small differences between edge and bulk are observed during the functionalization, beside the naturally occurring D-line between edge and bulk graphene, due to symmetry breaking at the edge. These small differences between edge and bulk could originate from the low amount of directly attached groups to the graphene plane camouflaging the higher edge reactivity.

The low induced defect density and high doping in this study could be an indication that the reaction conditions favoured building polymeric structures on the graphene surface binding directly to the surface. However, it should be noted that the low defect density might also be related to photoresist and other residues partly covering the graphene sheet after contacting and pattering the Hall bars reducing the area available for functionalization. So far, a high reactivity towards the diazonium chemistry has primarily been shown on non-processed graphene flakes.[15,16] On contacted graphene flakes, a previous study has also shown mainly doping effects in the bulk.[24] Only recently Zhang *et al.* showed on contacted (not etched by reactive ions) graphene samples that the addition of tetrabutylammonium hexafluorophosphate during the functionalization increases the reactivity towards the graphene surface, allowing to create more defects in the graphene plane.[20] However, the dopant concentration due to functionalization is significantly lower than what is observed in this work.

To further investigate the influence of chemical functionalization on electronic transport, we also performed transport measurements at a temperature of 4 K and a magnetic field up to 5 T. In Fig. 3(a) $R_{xx}$ as a function of $V_{BG}$ at 5 T is shown for the pristine device and after the first two functionalization steps. For the pristine device, clear magneto-oscillations can be seen, again pointing at the high quality of the untreated device. For increasing functionalization the oscillations are washed out. After the third functionalization step the mobility is lowered to 3700 cm$^2$ V$^{-1}$ s$^{-1}$ (see Fig. 1(c)) and the oscillations are not visible anymore. This is consistent with previous measurements of untreated devices of different mobilities.

In Fig. 3(b) the corresponding Schubnikov-de Haas oscillations measured at a density of $2.4 \times 10^{12}$ cm$^{-1}$ can be seen. The oscillations can be described by

$$\rho_{xx} = \frac{m}{ne^2\tau_D}\left[1 - 2e^{-\pi/\omega_c\tau_q}\frac{2\pi^2 k_B T/\hbar\omega_c}{\sinh(2\pi^2 k_B T/\hbar\omega_c)}\cos\left(\frac{j\pi hn}{2eB} - \phi\right)\right] - aB - bB^2 \quad (1)$$

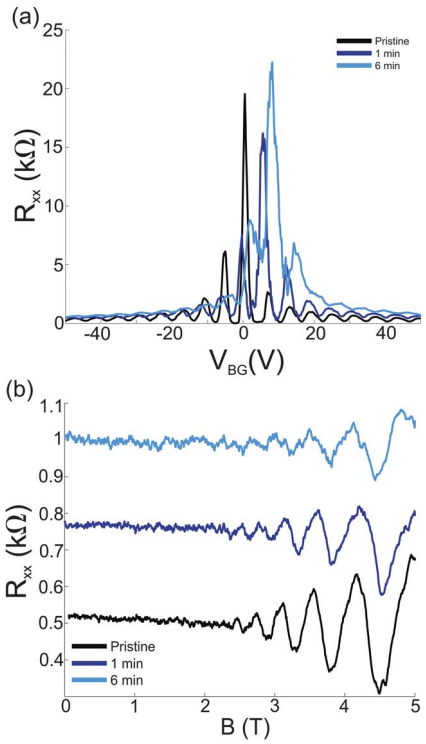


**Fig. 3** (a) $R_{xx}$ as a function of $V_{BG}$ at $B = 5$ T for the untreated graphene and the two first functionalization steps. (b) B-field dependence of $R_{xx}$ at $\Delta V_{BG} = -30$ V.

where $\omega_c = eB/m$ is the cyclotron frequency, $m = \hbar k_F/v_F$ is the cyclotron mass, and the two last terms describe the slightly decreasing background.[31] For graphene the phase $\phi$ is $\pi$ and $j = 1$.[32] By fitting the measurements shown in Fig. 3(b) with eqn (1) we extract the quantum scattering times $\tau_q$ and the Drude scattering times $\tau_D$ for the different functionalization steps. For the untreated graphene Hall bar we find $\tau_D = 181$ fs, $\tau_q = 67$ fs and $\tau_D/\tau_q = 2.7$. Correspondingly, we find $\tau_D = 120$ fs, $\tau_q = 47$ fs and $\tau_D/\tau_q = 2.55$ after 1 min functionalization and $\tau_D = 95$ fs, $\tau_q = 38$ fs and $\tau_D/\tau_q = 2.5$ after 6 min functionalization. From the fit we obtain a statistical uncertainty of $\pm 0.1$ for $\tau_D/\tau_q$. In addition, we have a significant systematic error. However, a thorough investigation of this error is beyond the scope of this paper. Both $\tau_D$ and $\tau_q$ decrease significantly with increasing functionalization time while their ratio $\tau_D/\tau_q$ decreases only slightly. From $\tau_D/\tau_q$, the nature of the induced scattering, long range or short range, can be extracted. A large ratio means that scattering is mainly in the forward direction, a result of long range scatterers, while $\tau_D/\tau_q \approx 2$ is a signature of short-range scatterers.[33] The $\tau_D/\tau_q$ ratios reported here are comparable to previously found ratios[32,34] and suggest that charged impurities close to the graphene sheet contribute most dominantly to scattering.[33] The fact that the individual scattering times $\tau_D$ and $\tau_q$ decrease significantly with functionalization while their ratio hardly changes, and the fact that the ratio obtained here is comparable to other pristine devices, is again an indication that the here-performed functionalization introduces scatterers for transport similar to dopants present from normal processing of samples.

## 4 Conclusions

The step-wise functionalized single layer graphene Hall bar devices were thoroughly characterized by Raman spectroscopy, RT and 4 K transport measurements. The Raman spectroscopy data shows that only few defects are introduced to the graphene structure. From both the Raman spectroscopy measurements and the transport measurements a clear doping effect is seen which exceeds the number of covalently bound moieties by one to two orders of magnitude. This suggests that the chemical reaction results in few covalent bound species, which then serve as seeds for a polymer-like growth using the diazonium ions as monomers.

## Acknowledgements

The authors thank C. Hierold for access to the Raman spectrometer, ETH Zurich and the Swiss National Science Foundation (SNF 206021-133768) for financial support.

## References

1 D. C. Elias, R. R. Nair, T. M. G. Mohiuddin, S. V. Morozov, P. Blake, M. P. Halsall, A. C. Ferrari, D. W. Boukhvalov, M. I. Katsnelson, A. K. Geim and K. S. Novoselov, *Science*, 2009, **323**, 610.
2 F. Withers, M. Dubois and A. K. Savchenko, *Phys. Rev. B: Condens. Matter Mater. Phys.*, 2010, **82**, 073403.
3 X. Hong, S. H. Cheng, C. Herding and J. Zhu, *Phys. Rev. B: Condens. Matter Mater. Phys.*, 2011, **83**, 085410.
4 M. Fang, K. G. Wang, H. B. Lu, Y. L. Yang and S. Nutt, *J. Mater. Chem.*, 2010, **20**, 1982–1992.
5 M. Y. Han, B. Ozyilmaz, Y. Zhang and P. Kim, *Phys. Rev. Lett.*, 2007, **98**, 206805.
6 Z. Chen, Y. Lin, M. Rooks and P. Avouris, *Phys. E.*, 2007, **40**, 228.
7 C. Stampfer, J. Guttinger, S. Hellmuller, F. Molitor, K. Ensslin and T. Ihn, *Phys. Rev. Lett.*, 2009, **102**, 056403.
8 E. McCann, *Phys. Rev. B: Condens. Matter Mater. Phys.*, 2006, **74**, 161403.
9 E. V. Castro, K. S. Novoselov, S. V. Morozov, N. M. R. Peres, J. M. B. Lopes dos Santos, J. Nilsson, F. Guinea, A. K. Geim and A. H. Castro Neto, *Phys. Rev. Lett.*, 2007, **99**, 216802.
10 J. B. Oostinga, H. B. Heersche, X. Lui, A. F. Morpurgo and L. M. K. Vandersypen, *Nat. Mater.*, 2007, **7**, 151.
11 Y. Zhang, T.-T. Tang, C. Girit, Z. Hao, M. C. Martin, A. Zettl, M. F. Crommie, Y. R. Shen and F. Wang, *Nature*, 2009, **459**, 820.
12 D. W. Boukhvalov and M. I. Katsnelson, *Phys. Rev. B: Condens. Matter Mater. Phys.*, 2008, **77**, 085413.
13 I. Zanella, S. Guerini, S. B. Fagan, J. Mendes Filho and A. G. Souza, *Phys. Rev. B: Condens. Matter Mater. Phys.*, 2008, **77**, 073404.
14 E. Bekyarova, M. E. Itkis, P. Ramesh and R. C. Haddon, *Phys. Status Solidi RRL*, 2009, **6**, 184.
15 F. M. Koehler, A. Jacobsen, K. Ensslin, C. Stampfer and W. J. Stark, *Small*, 2010, **6**, 1125–1130.
16 R. Sharma, J. H. Baik, C. J. Perera and M. S. Strano, *Nano Lett.*, 2010, **10**, 398.
17 E. Bekyarova, M. E. Itkis, P. Ramesh, C. Berger, M. Sprinkle, W. A. de Heer and R. C. Haddon, *J. Am. Chem. Soc.*, 2009, **131**, 1336.
18 F. M. Koehler, N. A. Luechinger, D. Ziegler, E. K. Athanassiou, R. N. Grass, A. Rossi, C. Hierold, A. Stemmer and W. J. Stark, *Angew. Chem., Int. Ed.*, 2009, **48**, 224.
19 A. Jacobsen, F. M. Koehler, W. J. Stark and K. Ensslin, *New J. Phys.*, 2010, **12**, 125007.
20 H. Zhang, E. Bekyarova, J.-W. Huang, Z. Zhao, W. Bao, F. Wang, R. C. Haddon and C. N. Lau, *Nano Lett.*, 2011, **11**, 4047.
21 C. Combellas, F. Kanoufi, J. Pinson and F. I. Podvorica, *Langmuir*, 2005, **21**, 280.
22 J.-H. Chen, C. Jang, S. Adam, M. S. Fuhrer and E. D. Williams, *Phys. Rev. Lett.*, 2008, **85**, 3476.

 

23 J.-H. Chen, W. G. Cullen, C. Jang, M. S. Fuhrer and E. D. Williams, *Phys. Rev. Lett.*, 2009, **102**, 236805.
24 D. B. Farmer, R. Golizadeh-Mojarad, V. Perebeinos, Y.-M. Lin, G. S. Tulevski, J. C. Tsang and P. Avouris, *Nano Lett.*, 2009, **9**, 388.
25 L. M. Malard, M. A. Pimenta, G. Dresselhaus and M. S. Dresselhaus, *Phys. Rep.*, 2009, **473**, 51.
26 C. Casiraghi, S. Pisana, K. S. Novoselov, A. K. Geim and A. C. Ferrari, *Appl. Phys. Lett.*, 2007, **91**, 233108.
27 C. Casiraghi, S. Pisana, K. S. Novoselov, A. K. Geim and A. C. Ferrari, *Appl. Phys. Lett.*, 2007, **91**, 241907.
28 L. G. Cancado, K. Takai, T. Enoki, M. Endo, Y. A. Kim, H. Mizusaki, A. Jori, L. N. Coelho, R. Magalhaes-Paniago and M. A. Pimenta, *Appl. Phys. Lett.*, 2006, **88**, 163106.
29 M. M. Lucchese, F. Stavale, H. Martins Ferreira, C. Vilani, M. V. O. Moutinho, B. R. Capaz, C. A. Achete and A. Jorio, *Carbon*, 2010, **48**, 1592.
30 M. Z. Hossain, M. A. Walsh and M. C. Hersam, *J. Am. Chem. Soc.*, 2010, **132**, 15399.
31 T. Ando, A. B. Fowler and F. Stern, *Rev. Mod. Phys.*, 1982, **54**, 438.
32 M. Monteverde, C. Ojeda-Aristizabal, R. Weil, K. Bennaceur, M. Ferrier, S. Guron, C. Glattli, H. Bouchiat, J. N. Fuchs and D. L. Maslov, *Phys. Rev. Lett.*, 2010, **104**, 126801.
33 E. H. Hwang and S. Das Sarma, *Phys. Rev. B: Condens. Matter Mater. Phys.*, 2008, **77**, 195412.
34 X. Hong, K. Zou and J. Zhu, *Phys. Rev. B: Condens. Matter Mater. Phys.*, 2009, **80**, 241415.